inter·noise 2021
1–5 August | Washington, DC

Innovative elastomeric shear leg mount concepts for quasi-zero stiffness isolation

Luke Fredette[1]
Cedarville University
251 N. Main St., Cedarville, OH 43140, USA

Rajendra Singh[2]
The Ohio State University
201 W. 19th Ave, Columbus, OH 43210, USA

ABSTRACT

Passive vibration isolation may be a cost-effective solution to isolate a supported system containing a source and/or receiver from the supporting structure. The standard linear theory suggests a low-stiffness joint to create a mobility mismatch in the transmission path, but this solution may lead to large amplitude motions in the supported system. To achieve both motion control and isolation with the same mount and without compromising either objective, an innovative, nonlinear mount concept is proposed. Taking advantage of geometric nonlinearity for large displacements, a quasi-zero stiffness is generated by exploiting the interaction between the nonlinear mechanisms that govern the motion of a number of inclined shear legs. For example, a three-regime stiffness profile is created, including a medium-stiffness preload regime, a quasi-zero stiffness isolation regime, and a high-stiffness motion control regime. This concept offers significant benefits compared with a more conventional compromise approach in that low-amplitude vibrations are exceptionally isolated while large amplitude transient motions are controlled. Illustrative computational examples are presented to support the underlying linear and nonlinear design principles. Limiting cases are discussed as well.

1. INTRODUCTION

Controlling structure-borne vibrations by reducing the path transmissibility may be an effective means of improving the noise, vibration, and harshness quality of vehicles. A conventional strategy to accomplish this goal in ground vehicle components (and other application spaces) is to design isolation elements with very low stiffness, typically as compliant joints between more rigid structural elements. These soft elements produce a mobility mismatch in the transmission path, which effectively reduces the transmissibility, as well documented in the literature [1-3]. However, the use of very compliant components in structural design may produce undesirable side-effects, such as increased motion amplitudes or reduced structural stability. This suggests the need for a nonlinear vibration isolator which can provide the desired low-stiffness property without compromising other requirements, and many configurations have been explored in the scientific literature [3].

A nonlinear isolation solution must be well-matched to the application for which it is designed. Most often, nonlinearity represents deviation from the well-known, predictable (linear) behavior of a

[1] lfredette@cedarville.edu
[2] singh.3@osu.edu

system, sometimes in a surprising way if the underlying assumptions have not been carefully formulated. To positively exploit nonlinearity, the designer must possess a detailed understanding of the physics, interactions between mechanisms, and operating (mean load) conditions. When these are harmonized, a nonlinear property may be a strong asset, yielding a degree of design success beyond the scope of any linear solution; however, a poor match between them will likely ruin the effectiveness of the design at best and may cause significant problems. The tuning of nonlinear features and interactions is therefore an important feature to ensure the utility and stability of an isolator design.

The application of tuned nonlinear behavior to a vibration isolation problem facilitates some highly beneficial possibilities. In particular, whereas the force or motion transmissibility of a component is directly related to its dynamic stiffness (including both storage and loss terms), the ideal stiffness of the component for isolation purposes would be zero. This is not practical for a linear solution, as it implies physically disconnecting the path, which is generally not possible while maintaining structural stability. In the context of a nonlinear design, however, the stiffness need not be zero for all operating points, but only at the crucial operating point wherein the isolation is required. Even then, it generally suffices to reduce the stiffness by one or more orders of magnitude, leading to the concept of a quasi-zero stiffness (QZS) property. Many approaches have been taken to achieve the QZS behavior [2 - 7], often involving the combination of geometric nonlinearities under large displacements or the buckling of beams. Many configurations rely on the interaction between a positive and negative stiffness element [5, 6], and the goal of this work is to build upon this foundation.

The chief goal of this article is to introduce an innovative QZS mount design idea that exploits a nonlinear interaction between axial and shear stiffness characteristics of a beam constructed from compliant materials to enhance vibration isolation without sacrificing motion control. First, a theoretical basis for the concept is laid out through the development of analytical, low-order models with discrete springs and continuous Euler beams. Second, the tuning of the design is explored and details are provided about which parameters might be useful to adjust the force and displacement limits. Finally, computational finite element models are used to verify the concept and analytical models and to ensure they reflect a viable physical mechanism.

2. THEORETICAL BASIS: NONLINEAR DESIGN CONCEPTS

A theoretical analysis of various nonlinear mechanisms establishes the framework for the present concept. Some nonlinear features are exploited, such as the geometric effect of large displacement, while others remain undesirable, like beam buckling.

2.1 Analytical Model for Discrete Springs

The first nonlinear mechanism used to construct the analytical model is the twin opposed inclined spring model (designated Model A in this paper) which is found in the literature in many variants [4]. A schematic of Model A is given in Figure 1 along with a plot of its stiffness characteristics, including a QZS regime near a displacement of $x = 0.45h$. The stiffness is determined (about the operating points) by computing the necessary applied force F to deflect the springs vertically by x,

$$F(x) = 2k(x-h)\left(1 - \sqrt{\frac{w^2+h^2}{w^2+(x-h)^2}}\right). \tag{1}$$

The effective stiffness of this system at any displacement x is computed ,

$$k_{e,A}(x) = \frac{\partial F}{\partial x} = 2k\left(1 - \sqrt{\frac{w^2+h^2}{w^2+(x-h)^2}} + \frac{(x-h)^2\sqrt{w^2+h^2}}{(w^2+(x-h)^2)^{3/2}}\right). \quad (2)$$

This mechanism produces a convenient decreasing stiffness which can be used to support a static load, but it vanishes as x approaches the critical value x_0 where $k_e \to 0$.

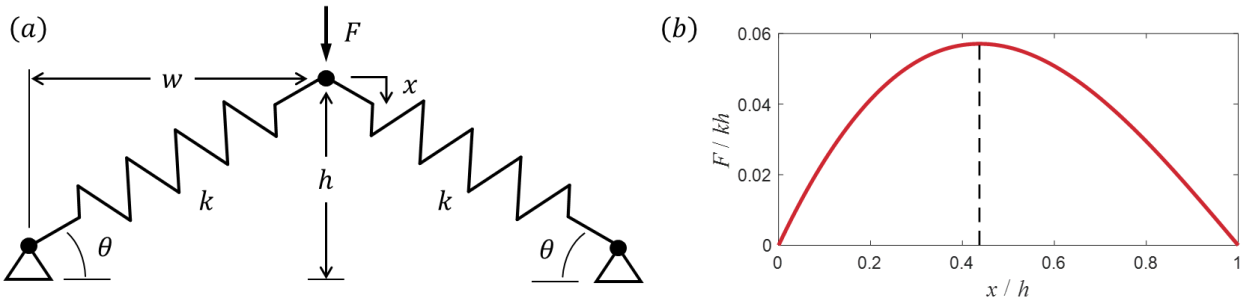

Figure 1: (*a*) A schematic of Model A with two inclined discrete springs and (*b*) its force-deflection property, exhibiting the geometric nonlinearity with both a positive and negative stiffness regime. Here, w is the radius of the isolator and h is the undeformed height.

2.2 Analytical Model for Inclined Euler Beams

While Model A represents a good first-order approximation of an isolation mount, the pinned connections shown in the model may not be physically feasible boundary conditions. Elastomeric materials are often used to achieve vibration isolation in a multitude of applications due to their low cost, low stiffness, and moderate damping. Using these materials, the displacement comes from flexure, which will have a corresponding stiffness. To account for this effect, the inclined lumped springs in Model A are replaced by inclined, cantilevered Euler beams (continuous elements) like the one shown in Figure 2. The pre-buckling axial force F_y is defined as follows where the y is the axial displacement as shown in Figure 2,

$$F_y = \frac{EA}{L} y \,, \quad (3)$$

where E is the elastic modulus of the material, A is the cross-sectional area, and L is the length of the beam. If the right end of the beam is pinned, the shear force is as follows where z is the transverse displacement of Figure 2 and I is the area moment of inertia of the cross-section,

$$F_z = \frac{3EI}{L^3} z \,. \quad (4)$$

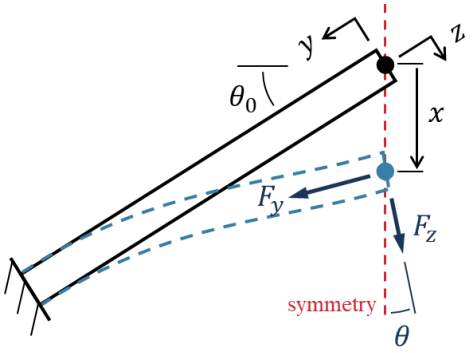

Figure 2. Inclined Euler beam with combined shear and axial deformations at the free end.

Here, If the right end is not free to rotate, as with a roller, the shear force increases as expressed below

$$F_z = \frac{12EI}{L^3} z. \tag{5}$$

The shear formulas in Equations 4 and 5 provide limiting cases for a realistic boundary condition, which may vary based on the real-life physical constraints. The configuration with two inclined beams is designated as Model B and is schematically depicted in Figure 3, along with the effective stiffness in terms of a force-deflection curve, exhibiting a relatively wide QZS regime near $x = 0.8h$. The force in Figure 3(b) is normalized by the product of E and A to provide a dimensionless reference for comparison across materials and bulk component size.

The behavior of the mount is governed by the combination of axial and shear stiffness terms. The axial stiffness of the shear leg is relatively high, but its contribution is diminished by nonlinear geometric transformation which occurs because the angle of inclination is a function of the linear displacement, $\theta = \theta(x)$. The vertical displacement x is transformed into axial and shear components (y and z, respectively), and then the linearized elastic equations (3) and (4) are applied to determine the forces in each direction. The vertical component of these are then combined to calculate F_x, given that the horizontal components must cancel due to symmetry. Following the algebra, the effective stiffness coefficient is expressed as,

$$k_{e,B}(x) = \frac{E}{L^3}\left(AL^2 \sin^2\left(\theta(x)\right) + 3I \cos^2\left(\theta(x)\right)\right). \tag{6}$$

The $\theta(x)$ term is critical in the decomposition of the vertical displacement x into its axial and shear components y and z and in the recombination of force components F_y and F_z into the resultant, F_x. Because of the linearization, the angles seen by each end of the beams are not the same. The left end of the beam pictured in Figure 2 is fixed, maintaining an angle of θ_0, while the slope of the right end is affected by the displacements. To accommodate the discrepancy in a linearized system context, the averaged angle between the undeformed orientation and the angle of the straight-line path between the base of the beam and the central node is used,

$$\theta(x) = \frac{1}{2}\left(\theta_0 + \tan^{-1}\left(\tan(\theta_0) - \frac{x}{L}\sec(\theta_0)\right)\right). \tag{7}$$

Although the large-displacement kinematics and shear mechanics of Model B tend to stiffen the mount compared to Model A, the shear stiffness fails to stabilize the model beyond the QZS regime. Both A and B exhibit negative stiffness behavior after x_0, which would likely cause a snap-through

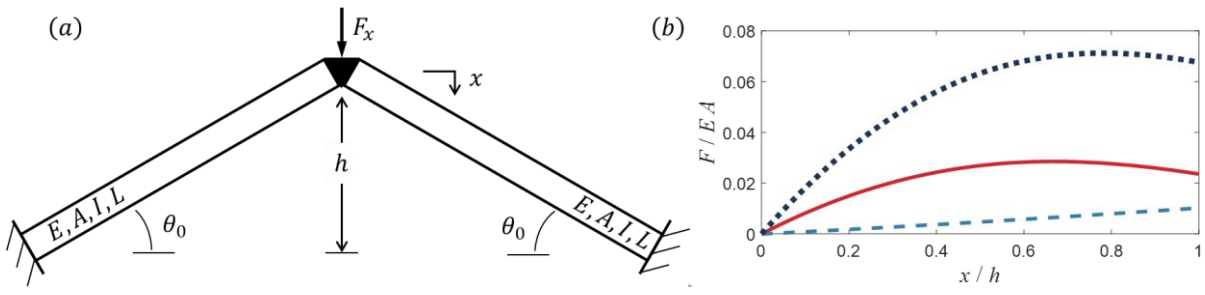

Figure 3. (a) Schematic representation of Model B with two inclined Euler beams (continuous elements) and (b) its force-deflection property, showing axial stiffness behavior similar to Model A with stiffening effects from the shear stiffness. Key: ——— - Axial force; - - - - Shear force; ▪▪▪▪▪ - Combined Force.

behavior that could destroy the mount and cause damage to the supported structure. Given the possibility of dynamic loading, this condition would almost certainly occur when operating in the QZS regime. A stabilizing element is therefore needed to provide motion control and prevent this catastrophic occurrence.

2.3 Inclusion of a Stopper

A stopper is introduced to the model to stabilize the large-displacement behavior. This element is a relatively stiff discrete spring in series with a clearance, which is precisely tuned to close when the shear legs are about to reach a negative stiffness. The stopper stiffness k_s is much larger than the slightly negative QZS, so the overall effective stiffness is maintained $k_e \geq 0$. This mechanism is defined as Model C and is shown schematically in Figure 4, along with the force-deflection property.

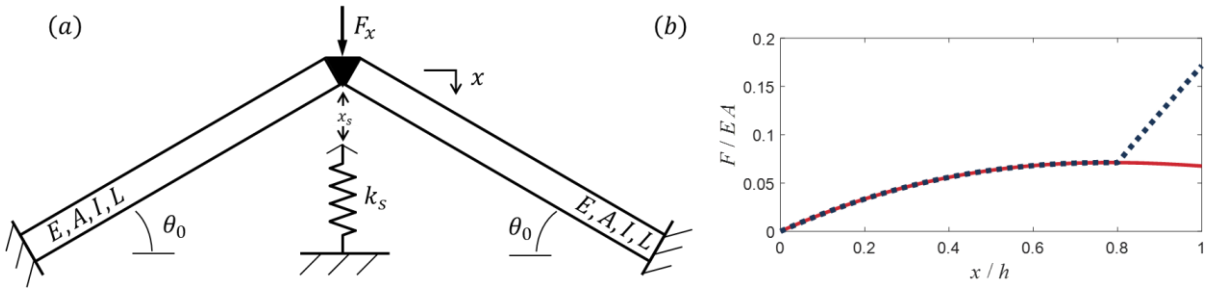

Figure 4. (a) Schematic representation of Model C with two inclined Euler beams (continuous elements) and a discrete spring (acting as a stopper) and (b) its force-deflection property, exhibiting the strong, positive stiffness from the quasi-zero stiffness regime produced by the stopper. Key: ——— - Model without stopper (Model B); ▪▪▪▪▪ - Model with stopper (Model C).

3. TUNING OF NONLINEAR MECHANISMS

The design concept proposed in this article works because of precise tuning between nonlinear mechanisms. In general, the axial stiffness in concert with the geometric nonlinearity (Model A, essentially) is the primary driver for QZS tuning because it is the mechanism which produces a negative stiffness. This feature controls $\theta(x)$, and is itself controlled by the values of θ_0 and L. Clearly, these two parameters will likely be bound by package space limitations.

The secondary tuning mechanism is the relative stiffening of the shear mechanics. Adding a positive shear stiffness shifts x_0 to the right and increases the overall load which may be supported by the mount in the QZS regime. The critical parameters for this mechanism are A and I, or in other words, the cross-section geometry. The A/I ratio is directly related to the aspect ratio of the cross-section. In this way, both the value of x_0 and the supported load may be affected: Increasing A and I together increases the supported load without adjusting the tuning, while adjusting them individually will influence x_0.

Finally, the influence of the material stiffness on the mount property may be observed in that k_e is proportional to E. Thus, a stiffer material will increase the overall load the mount supports in the QZS regime but should not appreciably affect the tuning.

Since the stopper has been included as a separate mechanism, its tuning should be defined only after the QZS regime has been tuned. Several factors should be considered. First, how much clearance should the stopper have? This is related to the desired operating range of the mount, which may be specified in terms of an operating point and dynamic range. This range should lie entirely in the QZS regime without overlapping with any negative stiffness or the stopper. Therefore, the stopper should engage at x_0 or before. Second, how stiff should the stopper be? This question depends on the

application. A stiff stopper can provide very good motion control but may generate large dynamic loads if it engages *in situ*. A compliant stopper may have better vibration properties but suffer from poor durability if it is insufficient to handle large transient loads. Third, how quickly does the stopper engage? A Boolean stopper engagement implies an abrupt change in stiffness from $k_e \approx 0$ to $k_e \approx k_s$, which may generate large impulsive loads in the system when transitioning between the QZS regime and the stopper regime. A stopper design which engages gradually may resolve this, but potentially at the cost of being insufficiently responsive to provide adequate motion control. Once again, the application must dictate these choices.

4. VERIFICATION USING A COMPUTATIONAL MODEL

While the low-order analytical models A, B, and C provide insights into the nonlinear physics of this QZS mount concept, they depend on a series of assumptions. These include Euler beam-like behavior of shear legs, assumptions about the boundary conditions of those beams, and the effectiveness of linearized beam stiffness equations in a large-displacement context. The physical validity of the underlying assumptions can be checked by conducting finite element simulations of this mechanism. By discretizing the material in relatively high resolution and simulating realistic boundary conditions, finite element models can verify whether the analytical model corresponds meaningfully to the physical mechanism. A finite element representation of Model C has been produced and is depicted in Figure 5.

To render Model C in a finite element context, certain practical adjustments are needed. In particular, the ends of the shear legs must be constrained to apply the load in a physically meaningful way. Some extra material is added to each end of the shear legs, allowing them to be couched in the fixture. This provides a way to apply the loads which could be experimentally validated in future work, but it also increases the effective length of the beam in the analytical model, $L_e = (1 + \delta)L$. The value of δ is empirically determined and found to be 11%. The effect end of the beam is 34% of the way through the added material. The δ parameter is a function of the boundary conditions, so any significant change in bonding conditions or geometric configuration may influence its value. In this case, contact is defined (with a friction coefficient of $\mu = 0.6$) between the interfacing parts, but no

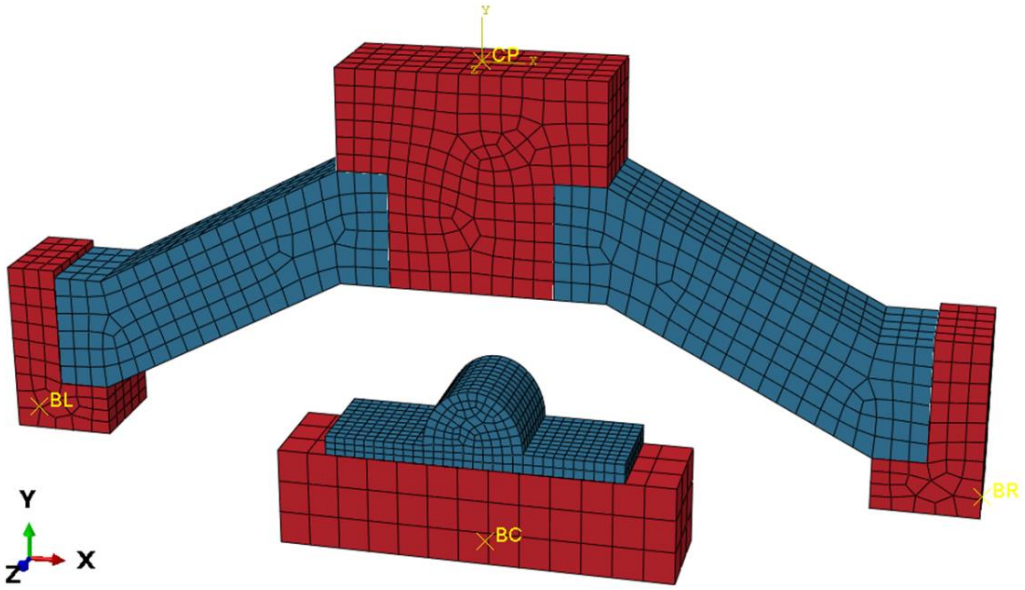

Figure 5. Finite element representation of mount Model C, with two shear legs and a stopper made of a soft rubber-like material and aluminum fixtures to enact realistic boundary conditions. Key: ■ - Aluminum fixture; ■ - Soft rubber-like material.

bonding. The resulting deflection at the upper fixture is therefore much more like a pinned connection than a fixed boundary condition, so the shear stiffness term in the analytical model uses Equation (4) rather than (5). A displacement input is applied to the upper fixture, and the reaction forces at the base of each shear leg fixture as well as the stopper base are all added together as the total transmitted force, F.

The resulting finite element deformation shape is shown in Figure 6, and the force-displacement curve is given in Figure 7. Reasonable physics are observed in the simulation, and excellent agreement is achieved between analytical and computational models, giving credence to the validity and utility of the design concept.

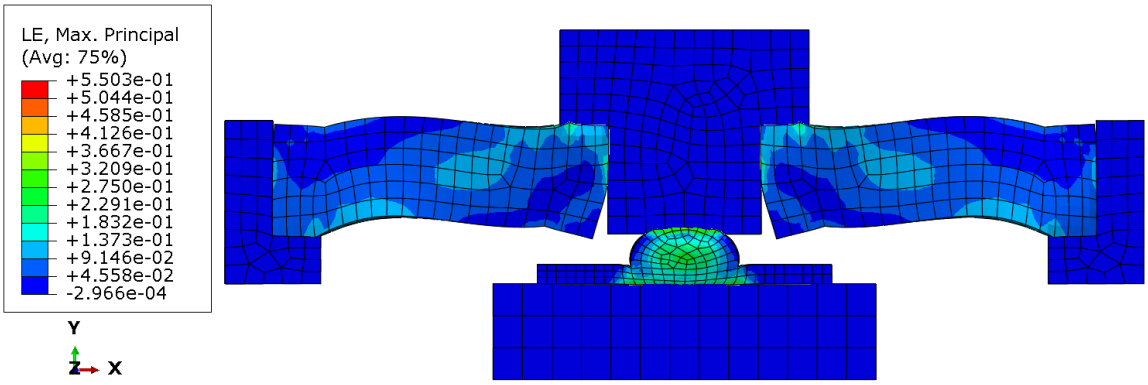

Figure 6. Deformed finite element model, illustrating the deflection shape of the inclined shear legs, the effects of unbonded boundary conditions, and the deformation of the stopper with maximum principal strain.

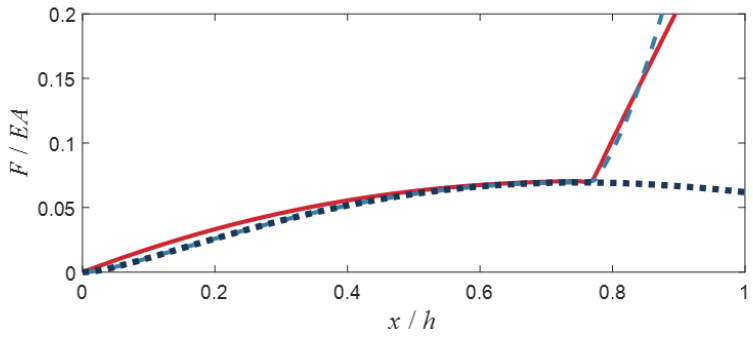

Figure 7. Comparison of computational and analytical models, showing a strong level of agreement in between the two methods. Key: ——— - Analytical Model C; - - - - Computational Model C; ▪▪▪▪▪ - Computational Model B (without stopper).

5. CONCLUSION

This article outlines a new isolator design concept which utilizes the nonlinear interaction between large-displacement shear and axial stiffness components of a compliant material. A theoretical foundation with several assumptions and simplifications is used to develop the concept. The analytical model predicts strong nonlinearity, so the relevant control parameters have been identified to adjust the load bearing capacity and isolation tuning. Computational verification has been undertaken using finite element models, and excellent agreement has been shown between the two methods. The resulting mount concept offers superior isolation to a mount design based on purely linear system principles while maintaining motion control to prevent large-amplitude motions. Future work is needed to develop this concept further, provide experimental validation, and translate the abstract concept to meet the specific needs of various application spaces.

5. ACKNOWLEDGEMENTS

We are grateful to the Ford Motor Company for supporting this work via the Ford-OSU Alliance program (2019-2021). Special thanks go to Y. Zhang, L. Liang, Y. Miao and P. Dhaval of the CAE-Cooling Module team for their contributions.

6. REFERENCES

1. Thomson, W. T. & Dahleh, M.D. *Theory of Vibration with Applications*, 5th Edition, Pearson, 1997.
2. Den Hartog, J.P. *Mechanical Vibrations*, 4th Edition, Dover, 1956.
3. Ibrahim, R.A. Recent advances in nonlinear passive vibration isolators. *Journal of Sound and Vibration*, **314**, 371-452 (2008).
4. Kovacic, I., Brennan, M.J., & Waters, T.P. A study of a nonlinear vibration isolator with a quasi-zero stiffness characteristic. *Journal of Sound and Vibration*, **315**, 700-711 (2008).
5. Meng, L., Sun. J., & Wu, W. Theoretical design and characteristics analysis of a quasi-zero stiffness isolator using a disk spring as a negative stiffness element. *Shock and Vibration*, (2015).
6. Zhao, F., Ji, J., Ye, K., & Luo, Q. An innovative quasi-zero stiffness isolator with three pairs of oblique springs. *International Journal of Mechanical Sciences*, **192**, 106093 (2021).
7. Liu, C., Yu, K. Accurate modeling and analysis of a typical nonlinear vibration isolator with quasi-zero stiffness. *Nonlinear Dynamics*, 2141-2165, (2020).